catalysts

MDPI

Article

Fragmentation-Oriented Design of Olefin Polymerization Catalysts: Support Porosity

Adriano G. Fisch

Department of Chemical and Materials Engineering, University of Alberta, Edmonton, AB T6G 2P5, Canada; fisch@ualberta.ca

Abstract: The development of catalysts for the production of polyethylene and polypropylene is ordinarily accomplished on a trial-and-error experimentation program. From the point-of-view of the fragmentation performance, support porosity is the key property affecting the mechanical support resistance, and, therefore, it determines the fragmentation process during the early moments of polymerization. The design of the support porosity can be more accurately determined by applying the theoretical knowledge acquired from previous research, but this is not consolidated for catalyst design. This article reports a methodology to optimize the support porosity using a simple fundamental model of the fragmentation process. Using this approach, the design of fragmentation-oriented supports can be achieved for polymerization reactors.

Keywords: Ziegler-Natta; metallocene; fragmentation; polyethylene; polypropylene

check for updates

Citation: Fisch, A.G. Fragmentation-Oriented Design of Olefin Polymerization Catalysts: Support Porosity. *Catalysts* **2023**, *13*, 160. https://doi.org/10.3390/catal13010160

Academic Editor: Carmine Capacchione

Received: 21 December 2022
Revised: 5 January 2023
Accepted: 9 January 2023
Published: 10 January 2023

1. Introduction

One remarkable feature of the heterogeneous polymerization process is the fragmentation of the fresh catalyst particle during the initial moments of the reaction [1–4]. Catalyst fragmentation is an essential step to guarantee the feasibility of the industrial process as it preserves the accessibility of the monomer to the active sites throughout the particle and prevents the generation of small polymer particles (fines) [1,2,5]. During the initial moments of the polymerization reaction, catalyst fragmentation occurs when the polymer recently accumulated in the pores creates a mechanical work against the wall that is beyond its ultimate strength [3,6,7]. At this moment, the pore wall cracks into smaller fragments, which typically range from 0.01 to 1 μm in size [1,5]. Two modes of fragmentation, layer-by-layer and continuous bisection, have been discriminated in the literature and experimentally observed for Ziegler-Natta catalysts [8]. Experiments have revealed that the mode of fragmentation is affected by the mass transfer occurring in the particle [9]. In the absence of strong mass transfer limitations, which are obtained when particle porosity is formed by larger pores, for example, the support disintegrates evenly by a layer-by-layer mechanism. The opposite favors the bisection mode of fragmentation. This implies that fragmentation is a dynamic phenomenon and, thereby, the monomer concentration gradient in the catalyst particle determines the front of fragmentation, as well as the fragmentation mode, along with other properties of the support and polymer.

Despite the steady evolution of the heterogeneous coordination catalysts since the work of Ziegler and Natta, the development of new synthetic routes, including new materials as supports, is still dependent on the trial-and-error approaches and the accumulated experience regarding the catalyst fragmentation performance. To improve this background, studies [7,9–11] have been conducted to evaluate and understand the effects of the support properties on catalyst fragmentation. These studies revealed the existence of a complex relationship between support properties, polymerization rate, and catalyst fragmentation. Distinct parameters are expected to influence the fragmentation, such as mechanical support strength, porosity, pore size distribution, polymer properties, the spatial distribution of

the catalytic sites in the support particle, and the polymerization rate. Different approaches have been used to model the fragmentation phenomenon [6] involving these variables. However, these studies were not devoted to the support design, and from the point of view of catalyst development, an increase in experimental efforts is needed in the absence of clear mathematical correlations between support properties and the fragmentation phenomenon. High-throughput experimentation has been employed as an alternative technique to reduce the experimental effort and to speed up the development of the support [12]. Overall, by the end of the development process, the prospective catalyst still needs to be tested regarding its fragmentation performance. Therefore, this represents a drawback in the research methodologies of heterogeneous coordination catalysis, which, if properly solved, could speed up the development of catalysts for olefin polymerization.

Considering the importance of catalyst fragmentation for the successful operation of the heterogeneous polymerization reactors, in this research work, a methodology to determine the support porosity and its relationship with the support material was developed from a phenomenological theoretical model. The potential benefits of this methodology were illustrated by two examples based on silica and magnesium dichloride as support materials.

2. Fragmentation Model

The relationship between the design variables of the catalyst and fragmentation during polymerization is analyzed by simplified theoretical models.

The local pressure against the pore wall is created by the progressive production of polymer and its consequential compression under confinement. The local pressure built-up in the pore can be derived from the formal definition of the polymer bulk modulus [6,13], as given in Equation (1).

$$P = K \ln\left(\frac{\rho_{conf}}{\rho_{free}}\right) \tag{1}$$

where K is the bulk modulus of the polymer, ρ_{free} is the specific mass of the polymer produced without any spatial restriction, and ρ_{conf} is the specific mass of the spatially confined polymer, which changes with time due to compression until an eventual fragmentation. The ratio between ρ_{conf} and ρ_{free} in Equation (1) represents the polymer densification (Π) due to the compression process.

Using the relation of Grüneisen-Tobolsky [13] (Equation (2)), the bulk modulus (K) of a semicrystalline polymer could be estimated as a function of the following properties: (i) cohesive energy (E_{coh}), (ii) molecular volume of the structural unit (v, Equation (3) for polyethylene), (iii) polymer fusion heat (ΔH_m), and (iv) polymer crystallinity content (χ, Equation (4)).

$$K = 8.04\left(\frac{E_{coh} + \chi \Delta H_m}{v}\right) \tag{2}$$

$$v = \frac{28}{\rho_{conf}} \tag{3}$$

$$\chi = \left(\frac{\rho_{conf} - \rho_a}{\rho_c - \rho_a}\right)\left(\frac{\rho_c}{\rho_{conf}}\right) \tag{4}$$

For high-density polyethylene (HDPE) with a density range of 940–980 kg m^{-3}, the value of K lies between 2.9 and 4.1 $\times$ 10^9 Pa.

The local mechanical energy stored by the compressed polymer (E) is then calculated from the pressure (P) as defined in Equation (5), in which V_{pore} is the pore volume of the catalyst particle.

$$\frac{\partial E}{\partial V_{pore}} = P \tag{5}$$

The mechanical resistance of the porous support mostly depends on both factors: the intrinsic resistance of the material and the porosity [14]. In other words, all formats of voids inside a given solid structure do not contribute to an increase in mechanical resistance but to its fragility. For porous materials, the mechanical resistance is determined by the solid skeleton. Considering this context, in this study, an extension of Griffith's model of fracture [15,16] is employed to predict the compressive strength of porous materials (Equation (6)).

$$\frac{\lambda(r)}{\lambda_o} = \left[\left(\frac{\phi_c - \phi(r)}{\phi_c}\right)^{1+m}\left(1 - \phi(r)^{\frac{2}{3}}\right)\right]^{\frac{1}{2}} \tag{6}$$

where λ_o, φ_c, and m are constants related, respectively, to the intrinsic compressive strength of the material, the critical porosity at the failure threshold, and the randomness degree of the pores (m = 1 for pores are randomly distributed; m < 1 for pores are clustered), and $\varphi(r)$ is the material porosity. The right-side term is then the correction of the intrinsic mechanical resistance of the material due to the porous structure.

The ultimate local energy supported by the pore wall (R) before cracking can be defined as a function of the compressive strength of the material [6], as expressed in Equation (7).

$$\frac{\partial R}{\partial V_{wall}} = \lambda(r) \tag{7}$$

where V_{wall} is the skeleton volume of the catalyst particle.

It is pertinent to define equations for both the pore volume (V_{pore}) and the wall volume (V_{wall}) considering a non-constant porosity ($\phi(r)$) as given:

$$\frac{\partial V_{pore}}{\partial V_{part}} = \phi(r) \tag{8}$$

$$\frac{\partial V_{wall}}{\partial V_{part}} = 1 - \phi(r) \tag{9}$$

where V_{part} is the volume of the catalyst particle.

The average porosity in the spherical particle, $\overline{\phi}$, can be calculated as:

$$\overline{\phi} = \frac{3}{{r_{part}}^3}\int_0^{r_{part}} \phi(r) r^2 dr \tag{10}$$

The fragmentation eventually occurs in a given radial position (r) of the catalyst particle when the resultant pressure caused by the polymer compaction on the pore wall (E) is beyond its compressive strength (R). This approach is stated from the equality of the accumulated energy by the compressed polymer and the ultimate support resistance, as given in Equation (11).

$$\frac{\partial E}{\partial r} = \frac{\partial R}{\partial r} \tag{11}$$

From the equality of Equation (11) and the definitions of Equations (5) and (7), it is possible to derive the fragmentation index expressed in Equation (12) considering a variable porosity ($\phi(r)$) along the particle radius (r). According to the defined index, fragmentation happens when $\Gamma_D \geq 1$. A detailed derivation of this fragmentation model is found in the Supplementary Material.

$$\Gamma_D = \frac{\frac{\partial E}{\partial r}}{\frac{\partial R}{\partial r}} = \left(\frac{\phi(r)}{1 - \phi(r)}\right)\left(\frac{P}{\lambda(r)}\right) \tag{12}$$

It is worth explaining that the proposed model predicts the occurrence of a local fragmentation, that is, in any radial position where the energy stored by the compressed polymer reaches the ultimate resistance of the pore skeleton (pore wall). Such a capability

allows the two mechanisms of fragmentation, layer-by-layer and continuous bisection, to be calculated when coupled to dynamic and spatial equations for the monomer transport in the catalyst particle and kinetic reactions [6,17].

To solve the proposed fragmentation model, it is imperative to determine the dependency of the porosity regarding the radial position in the catalyst particle. Unfortunately, the porosity profiles along the particle radius of polyolefin catalysts are unknown. Considering this background and the assumption of random distribution of pores in the particle [18], in this study, a random porosity with a Gaussian distribution (Equation (13)) is used to describe the radial porosity profile of the catalyst as described for concrete cement [19].

$$f(\phi) = \frac{1}{\sigma_\phi \sqrt{2\pi}} e^{-0.5\left(\frac{\phi-\overline{\phi}}{\sigma_\phi}\right)^2} \quad (13)$$

where σ_ϕ is the standard deviation, φ is the porosity, and $\overline{\phi}$ is the average porosity.

Different sets of parameters were used to generate the radial porosity profiles used in the simulations. Porosity profiles generated with $\overline{\phi}$ = 0.7–0.8 and σ_ϕ = 0.05 resemble the properties of precipitated, amorphous silica commonly used as supports. Alternatively, the porosity profiles generated setting $\overline{\phi}$ = 0.40–0.45 and σ_ϕ = 0.03 represent anhydrous magnesium dichloride supports. The random radial porosity profiles generated for these two materials, which are mostly used for polyolefin catalysts, are exemplified in Figure 1.

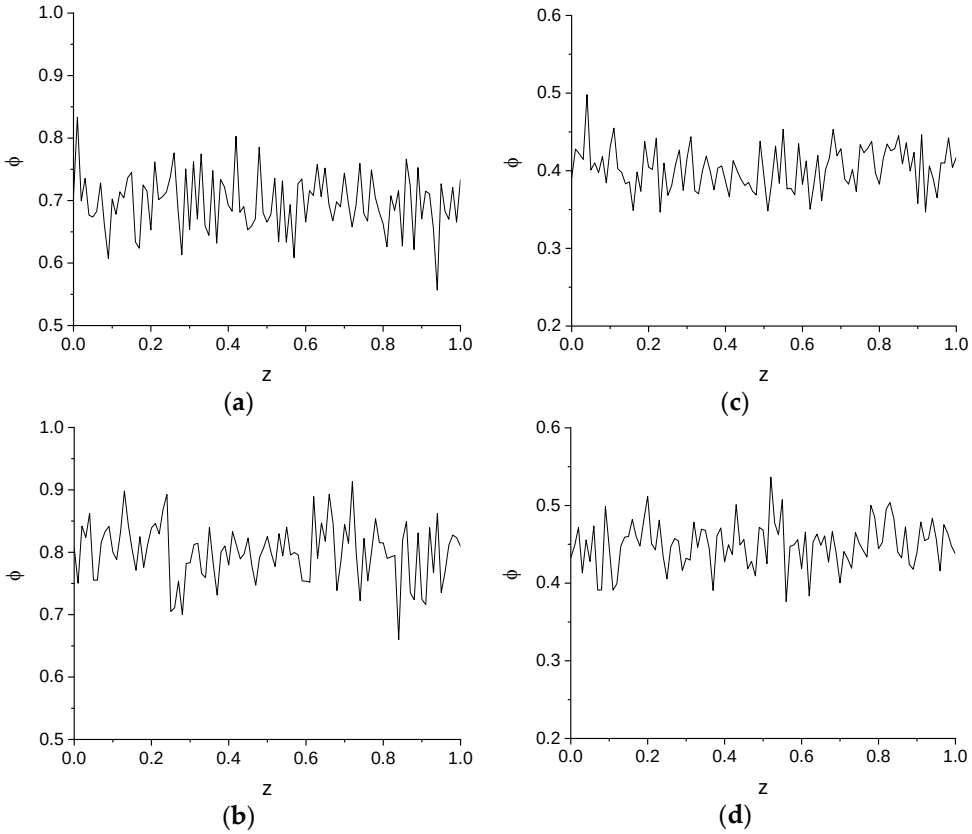

Figure 1. Random porosity distributions (φ) based on the normalized radial position (z) in the catalyst particle. (**a**) $\overline{\phi}$ = 0.7, σ_ϕ = 0.05. (**b**) $\overline{\phi}$ = 0.8, σ_ϕ = 0.05. (**c**) $\overline{\phi}$ = 0.4, σ_ϕ = 0.03. (**d**) $\overline{\phi}$ = 0.45, σ_ϕ = 0.03.

Additionally, the fragmentation model requires the setup of the intrinsic compressive strength (λ_o). For precipitated, amorphous silica, λ_o is around 1×10^9 Pa, while anhydrous magnesium dichloride is more fragile and has a lower value of λ_o, which can be speculated to be 1 or 2 orders of magnitude lower than the respective silica-based materials. As there

is no consensus in the literature, $\lambda_o = 1 \times 10^8$ Pa is set for anhydrous magnesium dichloride in this study.

3. Support Porosity Design

Particle porosity is an important feature of polyolefin catalysts once the monomer is distributed inside the particle through the pores. Apart from mass and heat transport, particle friability is another important aspect related to porosity [10,11,20]. Porous particles present a lower mechanical strength than the respective non-porous ones. In this sense, the porosity should be enough to induce a certain mechanical resistance to the particle; as such, its fracture happens as soon as the polymer fills up the pores, which means the fragmentation happens with minimal energy accumulation. In this scenario, the probability of the explosion of the particle during fragmentation due to the large accumulation of pressure energy in the particle is minimized. This is the argument used to determine the optimal porosity of the catalyst in this research.

Considering this context, limiting the polymer densification increase to 2% for the confined polymer density ($\Pi \leq 1.02$) seems to be enough to guarantee particle integrity during fragmentation. From the opposite point-of-view, the use of a lower limiting value for Π will require a more friable and consequently a more porous particle, which eventually cannot be manipulated properly during industrial operations of transport and transferring, for example, because of its fragile mechanical resistance. As the catalyst fragmentation process is not completely understood, the adoption of the limit $\Pi \leq 1.02$ is subject to scrutiny. However, this limiting value is suggested in this present research because of the absence of a better, justified one.

A map for the fragmentation of a catalyst particle is obtained by solving the system formed by Equations (1), (6), and (12) besides additional parameters λ_o, $\overline{\phi}$, and σ_ϕ for an adequate range of polymer densification (Π). With this model, a routine can be established to determine the adequate porosity for the support considering $\Gamma_D \geq 1$ and $\Pi \leq 1.02$ as a decision variable. This procedure is detailed in Figure 2.

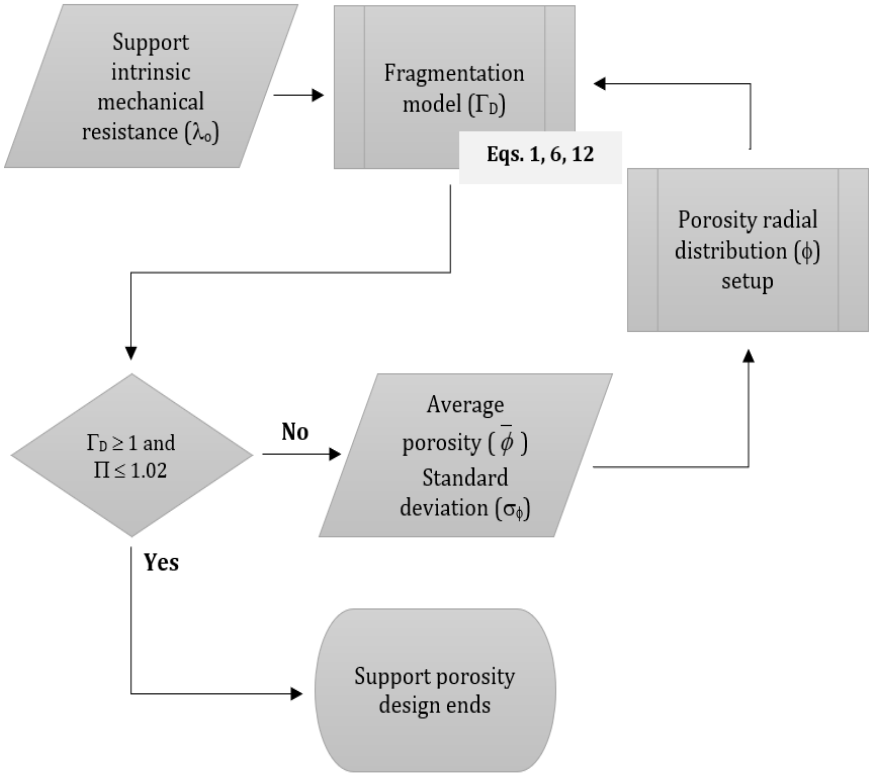

Figure 2. Routine for the design of the support particle.

Two examples are useful to illustrate this methodology for determining the support porosity. The first study deals with silica support which has an intrinsic mechanical resistance (λ_o) of 1×10^9 Pa. In Figure 3a, the map shows the profile of the fragmentation index (Γ_D) along the radial position of the particle for a support of 0.7 (70%) of average porosity. At a polymer densification lower than 1, the pore is not filled with polymer, and, therefore, no pressure energy is accumulated. From polymer densifications higher than 1, pressure energy builds up in the pores resulting, eventually, in a crack in the pore wall. As seen, most parts of the catalyst are fragmented with a maximum polymer densification of 1.02. The portions of the support that fragmented with lower polymer densification represent those regions of higher porosity and, consequently, lower material resistance. However, some portions of the catalyst are not fragmented, requiring more energy accumulation due to the higher material resistance in radial positions of lower porosity. For the design of a support that completely fragments within the limit $\Pi \leq 1.02$, the average porosity of the support needs to increase from 0.7 to 0.8, as indicated by the fragmentation map shown in Figure 3b. As it is noticed, the fragmentation index increases sharply with a support particle of lower mechanical resistance, which means that the force exerted by the polymer in the pores is higher than the ultimate mechanical resistance of the support as soon as the pores are full of polymer.

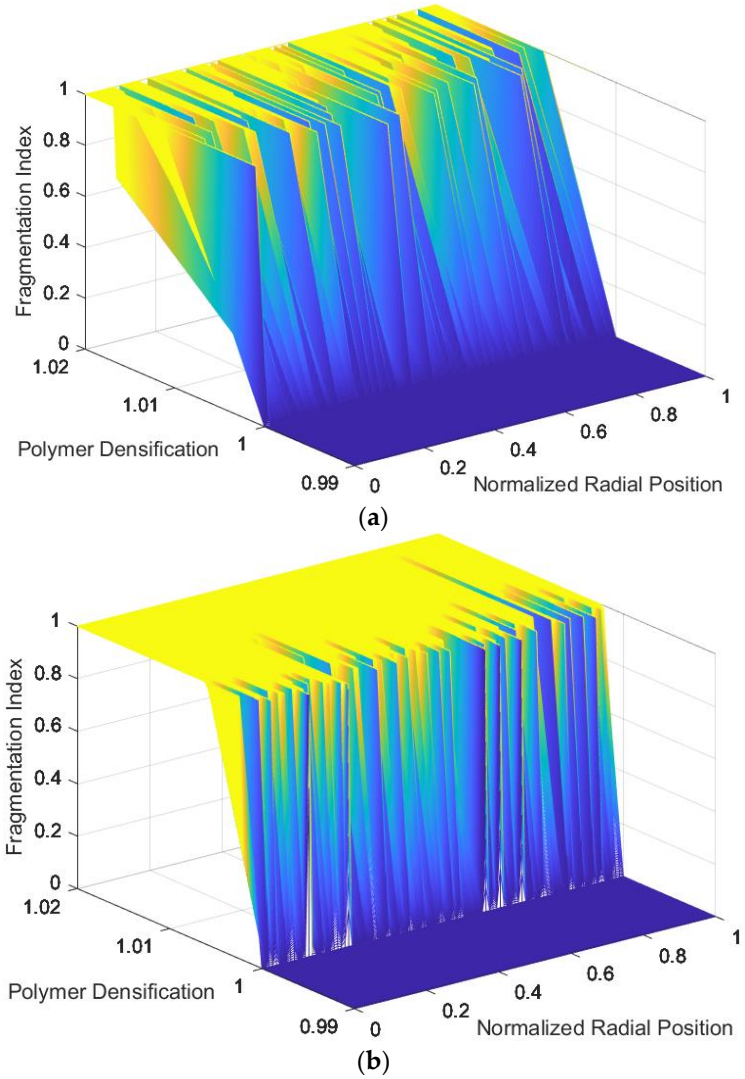

Figure 3. Fragmentation map for a support featuring: $\lambda_o = 1 \times 10^9$ Pa, (**a**) $\overline{\phi} = 0.7$, $\sigma_\phi = 0.05$, (**b**) $\overline{\phi} = 0.8$, $\sigma_\phi = 0.05$.

The use of a more friable material than SiO_2 as support, such as anhydrous magnesium dichloride, is also exemplified in this study. The intrinsic mechanical resistance of $MgCl_2$ used in this example is $\lambda_o = 1 \times 10^8$ Pa, one order of magnitude lower than that of SiO_2. For an average porosity of 0.4, the fragmentation map for $MgCl_2$ reveals that portions of the catalyst do not fragment within the limit $\Pi \leq 1.02$ (Figure 4a). However, increasing the average porosity from 0.40 to 0.45 decreases the mechanical resistance of the particle and, thereby, the support is fragmented within the required limit (Figure 4b).

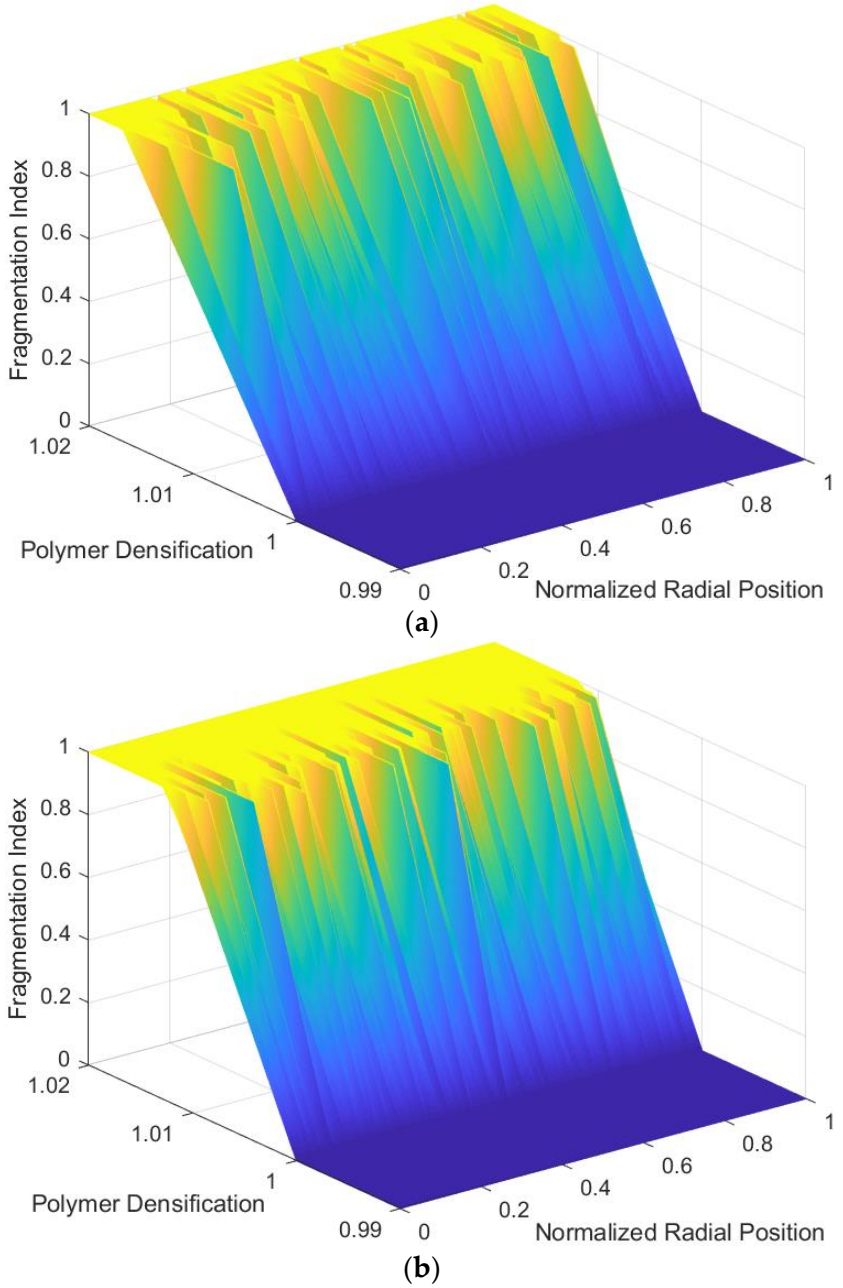

Figure 4. Fragmentation map for a support featuring: $\lambda_o = 1 \times 10^8$ Pa, (**a**) $\overline{\phi} = 0.40$, $\sigma_\phi = 0.03$, (**b**) $\overline{\phi} = 0.45$, $\sigma_\phi = 0.03$.

In these preceding examples, the average porosity was manipulated to attain the fragmentation of the whole support. As an additional parameter describing the porosity distribution in the particle, the porosity standard deviation (σ_ϕ) impacts the difference in the polymer densification between the regions of higher and lower porosities. This means

that, for a support particle with higher σ_ϕ, the complete fragmentation will happen with a higher densification gradient along the particle radius. This feature results in the sharp buildup of the fragmentation index because the average porosity needs to be high enough to guarantee the fragmentation within the limit $\Pi \leq 1.02$ for those catalyst portions of lowest porosity. This case is illustrated in the example of silica-based support (Figure 3b): the support portion at normalized radial position z = 0.8 required an average porosity of 0.8 for fragmentation.

It is not obvious, but the fragmentation with a high densification gradient has potential implications for the next step of polymerization, the polymer particle growth. Those regions of higher polymer density exhibit a higher mass transfer resistance which, in turn, can lead to a monomer concentration gradient in the particle. As a result, the catalyst activity is reduced, and the molecular weight distribution of the polymer is broadened. It is easy to extend the effects of the high densification gradient to heat transfer, which can result in hot spots inside the particle with the potential to accelerate the active site deactivation, for example.

In fact, the standard deviation is not actually a feature the researcher can effectively pick from a shelf, but it is an intrinsic characteristic of the material with which he has to deal with. The average porosity is the opposite, and there are many options available on the market. In this context, the practical property manipulated in the design of the support is the average porosity in most cases. For further advances, studies are necessary to shed light on the limits and implications of the porosity standard deviation of the support particle.

The average porosities calculated to obtain fragmented support particles for these two examples agree with the experimental data [21]. For the synthesis of SiO_2-based Ziegler−Natta catalysts, particle porosity ranging from 0.7 to 0.9 is commonly employed, while for $MgCl_2$-based catalysts, the porosity ranges from 0.4 to 0.6. This validates the model and the methodology for further use and extensions to other systems.

From another point of view, it is also important to highlight that, from the polymerization process side, it is decisive to guarantee the support fragmentation but not the mode it happens, layer-by-layer or bisection or even a combination of these modes. Thereby, it is not necessary to predict the mode of fragmentation to design the porosity of the support.

4. Methodology Potential

It is worth noticing that the presented methodology calculates the polymer densification required for the catalyst fragmentation in a given radial position. It is also important to recall that polymer production is a dynamic phenomenon; that is, it is time-dependent, and so is the fragmentation process. In this condition, the time to produce the required polymer in order to crack the support is different for every radial position, which relies on the transport of the monomer in the particle. In this regard, the fragmentation model developed in this research can be associated with dynamic models for mass and energy balances to create a mathematical tool for modeling pre-polymerization reactors. This model can be further used for optimizations of additional properties of the support particle, such as the particle size and pore size distributions.

In the preceding examples, the average support porosity was optimized for materials such as amorphous silica and anhydrous magnesium dichloride. The potential use of alternative materials implies the need for a long-term research program in which tests in pilot plants are required to determine the feasibility of the proposed support to fragmentation. In this context, the developed model can speed up the design of the properties of alternative support materials in terms of fragmentation.

5. Conclusions

From the point-of-view of the catalyst design, support porosity has a direct influence on the mechanical resistance of the catalyst particle, and due to this, it represents an important aspect of the fragmentation behavior. In the research reported in this article, a simple phenomenological mathematical model was developed and used to determine

the support porosity considering the mechanical resistance of the support material. The porosity calculated by the model is comparable to reference data for both silica and magnesium dichloride supports, and the design approach presented can reduce the reliance on experiments and expedite the research activities in the development of polyolefin catalysts, including the research of alternative supports to SiO_2 and $MgCl_2$.

Supplementary Materials: The following supporting information can be downloaded at: https://www.mdpi.com/article/10.3390/catal13010160/s1, Deduction of Equation (12).

Funding: This research received no external funding.

Data Availability Statement: No new data were created or analyzed in this study. Data sharing is not applicable to this article.

Conflicts of Interest: The author declares no conflict of interest.

References

1. Soares, J.B.P.; McKenna, T.; Cheng, C.P. Coordination Polymerization. In *Polymer Reaction Engineering*; Asua, J.M., Ed.; Blackwell Publishing Ltd.: Oxford, UK, 2007; pp. 29–117.
2. Soares, J.B.P.; Mckenna, T.F. *Polyolefin Reaction Engineering*; Wiley-VCH: Weinheim, Germany, 2012.
3. Kazerooni, N.M.; Eslamloueyan, R.; Biglarkhani, M. Dynamic simulation and control of two-series industrial reactors producing linear low-density polyethylene. *Int. J. Ind. Chem.* **2019**, *10*, 107–120. [CrossRef]
4. Bossers, K.W.; Valadian, R.; Garrevoet, J.; van Malderen, S.; Chan, R.; Friederichs, N.; Severn, J.; Wilbers, A.; Zanoni, S.; Jongkind, M.K.; et al. Heterogeneity in the Fragmentation of Ziegler Catalyst Particles during Ethylene Polymerization Quantified by X-ray Nanotomography. *JACS Au* **2021**, *1*, 852–864. [CrossRef] [PubMed]
5. van der Ven, S. *Polypropylene and Other Polyolefins*; Elsevier: Amsterdam, The Netherlands, 1990.
6. Fisch, A.G.; Dos Santos, J.H.Z.; Secchi, A.R.; Cardozo, N.S.M. Heterogeneous Catalysts for Olefin Polymerization: Mathematical Model for Catalyst Particle Fragmentation. *Ind. Eng. Chem. Res.* **2015**, *54*, 11997–12010. [CrossRef]
7. Emami, M.; Parvazinia, M.; Abedini, H. Gas-phase polymerization of propylene at low reaction rates: A precise look at catalyst fragmentation. *Iran. Polym. J.* **2017**, *26*, 871–883. [CrossRef]
8. Bossers, K.W.; Valadian, R.; Zanoni, S.; Smeets, R.; Friederichs, N.; Garrevoet, J.; Meirer, F.; Weckhuysen, B.M. Correlated X-ray Ptychography and Fluorescence Nano-Tomography on the Fragmentation Behavior of an Individual Catalyst Particle during the Early Stages of Olefin Polymerization. *J. Am. Chem. Soc.* **2020**, *142*, 3691–3695. [CrossRef] [PubMed]
9. Werny, M.J.; Zarupski, J.; Have, I.C.T.; Piovano, A.; Hendriksen, C.; Friederichs, N.H.; Meirer, F.; Groppo, E.; Weckhuysen, B.M. Correlating the Morphological Evolution of Individual Catalyst Particles to the Kinetic Behavior of Metallocene-Based Ethylene Polymerization Catalysts. *JACS Au* **2021**, *1*, 1996–2008. [CrossRef] [PubMed]
10. Hammawa, H.; Wanke, S.E. Influence of support friability and concentration of α-olefins on gas-phase ethylene polymerization over polymer-supported metallocene/methylaluminoxane catalysts. *J. Appl. Polym. Sci.* **2007**, *104*, 514–527. [CrossRef]
11. Vakili, M.; Arabi, H.; Mobarakeh, H.S. The effect of SiO_2 porosity on activity profiles and comonomer incorporation in slurry ethylene/butene-1 polymerization by (SiO2/MgCl2/TEOS/TiCl4) catalyst system. *J. Appl. Polym. Sci.* **2012**, *124*, 5145–5153. [CrossRef]
12. Chammingkwan, P.; Terano, M.; Taniike, T. High-Throughput Synthesis of Support Materials for Olefin Polymerization Catalyst. *ACS Comb. Sci.* **2017**, *19*, 331–342. [CrossRef] [PubMed]
13. Van Krevelen, D.W.; Te Nijenhuis, K. *Properties of Polymers, Their Correlation with Chemical Structure; Their Numerical Estimation and Prediction from Additive Group Contributions*, 4th ed.; Elsevier: Amsterdam, The Netherlands, 2009; p. 209.
14. Biswas, D.R. *Influence of Porosity on The Mechanical Properties of Lead Zirconate–Titanate Ceramics*; University of California: Bekerley, CA, USA, 1976. [CrossRef]
15. Chen, X.; Wu, S.; Zhou, J. Influence of porosity on compressive and tensile strength of cement mortar. *Constr. Build. Mater.* **2013**, *40*, 869–874. [CrossRef]
16. Griffith, A.A., VI. The phenomena of rupture and flow in solids. *Philos. Trans. R. Soc. Lond. Ser. A* **1921**, *221*, 163–198.
17. Dos Santos Boll, B.; Dutra, C.P.; Santos, J.H.Z.; Fisch, A.G.; Cardozo, N. Experimental Evaluation of a Catalyst Fragmentation Model for Olefin Polymerization. *Macromol. React. Eng.* **2020**, *14*, 2000008. [CrossRef]
18. Sheikhzadeh, M.; Pourmahdian, S. A Multipore Model for Heterogeneous Catalytic Polymerization: Structure–Performance Relationships. *Macromol. React. Eng.* **2022**, *16*, 2100021. [CrossRef]
19. Martin, W.D.; Putman, B.J.; Kaye, N.B. Using image analysis to measure the porosity distribution of a porous pavement. *Constr. Build. Mater.* **2013**, *48*, 210–217. [CrossRef]

20. McDaniel, M.P. Influence of Catalyst Porosity on Ethylene Polymerization. *ACS Catal.* **2011**, *1*, 1394–1407. [CrossRef]
21. Kissin, Y. *Alkene Polymerization Reaction with Transition Metal Catalysts*; Elsevier: Amsterdam, The Netherlands, 2008.